Reduced Stiffness Buckling Analysis of Aboveground Storage Tanks with Thickness Changes

by

Rossana C. Jaca, Luis A. Godoy, and James G.A. Croll

Reprinted from

Advances in Structural Engineering

Volume 14 No. 3 2011

MULTI-SCIENCE PUBLISHING CO. LTD.
5 Wates Way, Brentwood, Essex CM15 9TB, United Kingdom

Reduced Stiffness Buckling Analysis of Aboveground Storage Tanks with Thickness Changes

Rossana C. Jaca[1], Luis A. Godoy[2,*], and James G.A. Croll[3]

[1]Constructions Department, Universidad Nacional del Comahue, Neuquén, Argentina
[2]Structures Department, FCEFyN, Universidad Nacional de Córdoba and CONICET, P.O. Box 916 (Correo Central), Córdoba, Argentina
[3]Department of Civil, Environmental and Geomatic Engineering, University College London, Gower Street, London WC1E 6BT, UK

(Received: 1 March 2010; Received revised form: 31 August 2010; Accepted: 27 September 2010)

Abstract: The Reduced Stiffness Analysis (RSA) to compute lower bounds to buckling loads of shells has been employed by a number of researchers as a simple way to evaluate the buckling capacity of shells that display unstable behavior and imperfection-sensitivity. It allows the use of simple eigenvalue analysis, without having to perform incremental nonlinear analysis, and is based on the physical behavior of the shell which recognizes that a significant contribution to the stability of a shell under lateral pressure is provided by its membrane stiffness. Unstable post-critical behavior is associated with the loss of this stabilizing membrane contribution. Past use of the approach has been mainly restricted to cases of uniform shell thickness and uniform pressures in the circumferential direction, in which case analytical solutions are possible. Recent applications by the authors and other researchers have shown ways to compute the lower bounds using finite element analysis, for which a modified eigenvalue analysis is constructed by neglecting the membrane contributions to the matrix containing the initial stresses. This paper illustrates the application of the methodology to cases of pressure loaded shells with thickness changes in the meridional direction. A semi-analytical finite element code has been employed for the buckling analysis when uniform pressures act on aboveground steel tanks. The tanks are representative of those constructed for the oil industry, with diameter to thickness ratios of the order of 3000, and height to diameter ratios lower than one.

Key words: buckling, elastic stability, shells, tanks, thin-walled structures.

1. INTRODUCTION

The theory of Reduced Stiffness Analysis (RSA) to obtain lower bound buckling loads (or reduced energy approach, as it has been termed in some publications) was first proposed 35 years ago (Croll 1975) as an attempt to account for the intriguing imperfection-sensitive behavior of shells. The approach was based on earlier work published by Donnell (1934) on the coupling between modes of instability and geometric imperfections. Croll proposed that part of the contribution to the elastic energy of the structure was eroded as a consequence of such coupling, with the consequence that the effective contribution to the stability of the shell was less than what would be computed in a classical analysis. Therefore, a lower bound to the buckling load of an imperfection-sensitive shell could be obtained by means of an eigenvalue analysis of the perfect shell in which the at risk, initially stabilizing, energy components have been eliminated (see for example Croll 1995). The identification of what terms need to be eliminated in each specific case was part of the development of the theory during the past 30 years. Under lateral pressure, it was found that the membrane energy provides the at-risk stabilizing terms and should be subsequently neglected for the reduced stiffness eigenproblem (Batista and Croll, 1978). A

*Corresponding Author. Email address: lgodoy@com.uncor.edu. Tel: +54-351-433-4144.

clear advantage of this approach is that rather than performing a geometrically nonlinear analysis for shells with various imperfection shape and amplitudes, the reduced stiffness methodology performs simpler computations by means of a modified eigenvalue analysis. Such an approach allows rapid estimates of shell buckling loads to be found and could be important in at least two situations: (i) to estimate elastic (or elasto-plastic) buckling of a specific shell; and (ii) to compute the buckling capacities of a large number of shells, as is required in the investigation of the consequences of a possible regional event, such as in the development of fragility or vulnerability curves (Khanduri & Morrow 2003; HAZUS 2003).

During the first decade of the research program, the investigations focused on the behavior of thin-walled cylinders under axial load and under uniform lateral pressure, leading to effective lower bounds with respect to data obtained from small scale experiments. Those applications were followed by studies on hyperboloids of revolution, spherical shells, domes, and stiffened shells (for a summary of progress in this research program, see Croll 1995). In most cases, the reduced energy models were solved analytically for simple boundary conditions, or else using special purpose numerical methods. With an increased number of applications, new challenges emerged that needed to be addressed. This paper is motivated by the need to represent the buckling of shells with thickness changes along the meridian, which is a common situation in the structural analysis of storage tanks employed in the oil industry.

Metal shells used to store liquids, such as aboveground storage tanks, are usually designed with step-changes in the thickness to resist fluid pressures (which are maximum at the bottom of the tank and zero at the top). The usual practice in this industry is to fabricate tanks using curved plates with standard dimensions, so that 8 ft. (2.67 m) rings are welded on top of each other. For an effective use of the reduced stiffness approach to the buckling of such shells, several questions arise. Should the reduction of stiffness (or energy) be enforced on the complete shell or on part of it? What terms should be eliminated in any case? Notice that this problem is not present in shells with constant thickness under uniform states of stress. Similar questions would arise in the buckling of shells formed by cylinder-cone or cylinder-dome configurations.

Several approaches have been proposed to evaluate the buckling capacity of stepwise variable wall thickness in shells. Early work in this field was done by Trahair *et al*. (1983) in Australia, followed by Rotter and Teng (1989), and Greiner and Yang (1996). The recent European recommendations (Rotter and Schmidt 2008) include a chapter on this topic because of its importance for the design of tanks and (to a lesser extent) of silos which become vulnerable to buckling under wind loading when empty. The intention of the European recommendations is to provide simple rules for designers so that buckling calculations can be made by hand.

In this paper we focus our attention on the cylindrical shell under uniform external pressure (or internal vacuum), and explore possible ways to implement a RSA under such conditions. As such, the paper emphasizes methodological rather than design issues. The effects of possible plastic strains are neglected in this study, since in general plasticity is not a dominant effect for such thin shells.

2. CANTILEVER SHELLS WITH STEPWISE THICKNESS CHANGES

Figure 1 schematically shows the domain of a structure divided in two zones with different stiffnesses, in which zone 2 is assumed to have larger stiffness than zone 1 as a consequence of their different thicknesses (with $t_2 > t_1$).

Using the total stiffness as derived from classical Love-Kirchhoff shell theory, a finite element model of the problem leads to the linear equilibrium condition valid for pre-critical states:

$$\mathbf{K_0}\,\mathbf{u}^F + \lambda^F \mathbf{P} = 0 \tag{1}$$

where $\mathbf{K_0}$ is the linear stiffness matrix of the shell, $\mathbf{u}^F$ is the vector of nodal displacements, λ^F is the load parameter along the fundamental linear equilibrium path, and $\mathbf{P}$ is the load vector. Using standard finite element notation (Zienkiewicz and Taylor 2005), the stiffness matrix $\mathbf{K_0}$ is computed in terms of matrix $\mathbf{B_0}$ which includes the interpolation functions and the constitutive matrix $\mathbf{D}$ computed from the material properties:

$$\mathbf{K_0} = (\mathbf{B_0}^T \mathbf{D} \mathbf{B_0})\,\mathrm{d}A \tag{2}$$

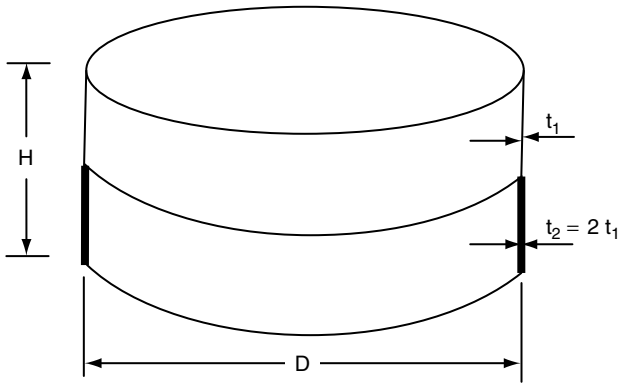

Figure 1. Tank structure with two different thicknesses

The stiffness matrix $\mathbf{K_0}$, for small deflections can be conceptualized as formed by membrane and bending contributions. With the resulting values of displacements obtained from the solution of Eqn 1, it is possible to compute the vector of stress resultants in the pre-critical condition, denoted as $\mathbf{N^F}$.

Various ways of performing stability analysis of shells using global numerical analysis have been recently reviewed in a European document (Rotter and Schmidt 2008). In a classical Linear Bifurcation Analysis (LBA), the resulting eigenvalue problem may be written in the form (Zienkiewicz and Taylor 2005, Chapter 17):

$$\left[\mathbf{K_0} + \lambda^C \mathbf{K^G}(\mathbf{N^F})\right]\mathbf{\Phi} = 0 \tag{3}$$

where λ^C is the critical load, and $\mathbf{\Phi}$ is the eigenvector that represents the deflected shape at the critical state. Matrix $\mathbf{K^G}$ includes the nonlinear components of rotations through matrix $\mathbf{G}$ (the rotation-displacement matrix) and it also includes the initial stresses computed from the fundamental equilibrium path, $\mathbf{N^F}$:

$$\mathbf{K}^G = (\mathbf{G}^T \mathbf{N}^F \mathbf{G})\,dA \tag{4}$$

A semi-analytical finite element has been used in this work (Flores and Godoy 1991) to model the classical and reduced stiffness models, whereas the general purpose program ABAQUS (2002) was employed for the geometrically nonlinear analysis of shells including imperfections in the geometry (GNIA, as identified in Rotter and Schmidt 2008).

In the precritical states, the largest contribution to the stiffness in thin-walled structures is provided by the membrane action. For tanks with height to diameter ratio close to one (H/D (1), the thickness designed according to API 650 recommendations (API 1988) lead to values at the bottom which are 3.5 to 4 times the thickness at the top of the shell. For this reason the stiffness contributions associated with regions at the bottom of the shell are larger than those at the top. Based on this kind of consideration, some authors propose to model only the thinner part of the shell by assuming an equivalent shell of uniform thickness supported by the thicker part. However, this is only a heuristic argument and the results need to be further justified since they may not be close to the values computed from an exact model of the shell.

2.1. Results of Classical LBA and GNIA Models

To illustrate the differences between the classical and reduced stiffness methods, a cantilever steel shell with two thicknesses has been initially considered under uniform external pressure. The boundary conditions are assumed as a free edge at the top, a condition identified as BC3 in European Design Recommendations (Rotter and Greiner 2008) and clamped at the bottom, or BC1r in the European Design Recommendations. There is no axial restraint included in the boundary conditions of the models discussed in this paper. With reference to Figure 1, the shell considered has D = 9 m, H/D = 0.5, with the largest thickness t_2 = 6 mm over the bottom half corresponding with D/t_2 = 1500 and the smaller thickness t_1 = 3 mm over the top half being D/t_1 = 3000. Values of elastic modulus E = 206000 MPa and Poisson's ratio equal to 0.3 for steel have been considered in the studies of this paper.

The classical eigenvalue problem was solved using the general purpose finite element program ABAQUS (2002) and also with the semi-analytical finite element

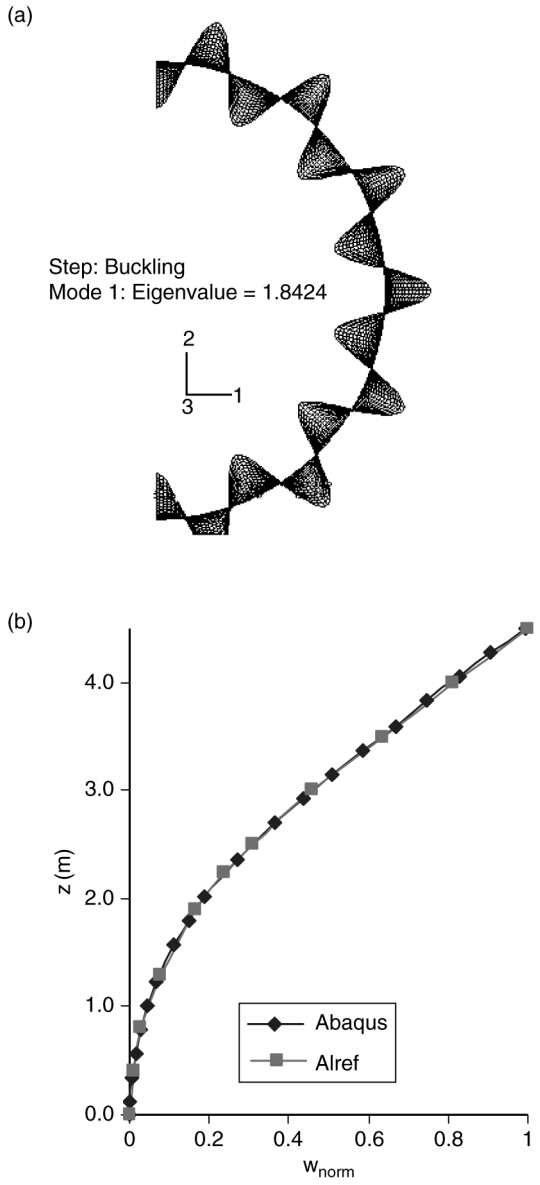

Figure 2. First classical buckling mode for the structure of Figure 1: (a) in the circumferential direction; (b) in the longitudinal direction

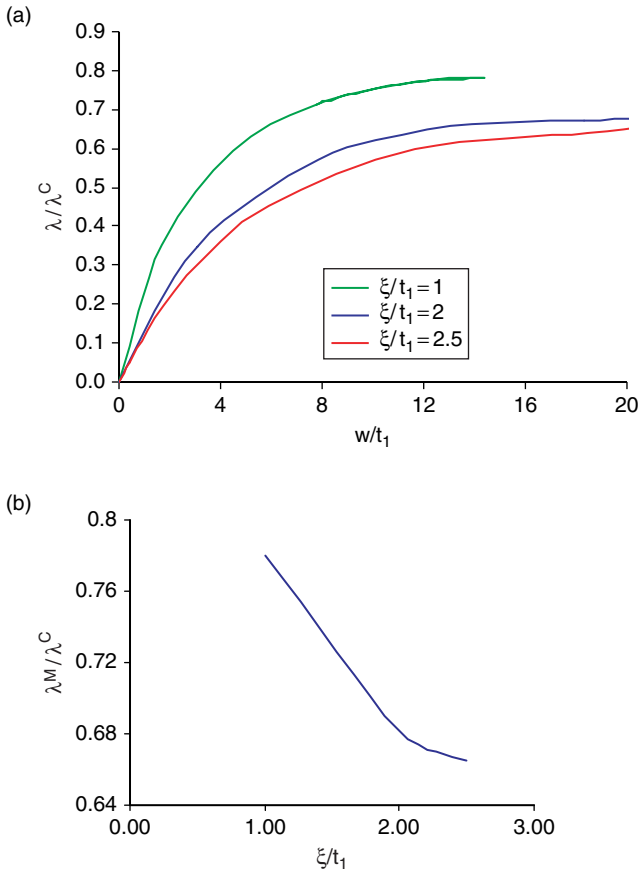

Figure 3. (a) Non-linear equilibrium paths, w is the out of the plane displacement at the point of largest displacement; (b) imperfection sensitivity curve (λ^C = 1.84 kPa)

code ALREF (Flores and Godoy 1991), leading to a value λ^C = 1.84 KPa. The deflected shape at λ^C computed from the eigen-problem is shown in Figure 2, where z is the coordinate measured along the meridian of the shell, and w_{norm} indicates the out-of-plane displacement normalized so that the maximum displacement (at the top in this case) has unit value.

Next, a Geometrically Nonlinear Imperfect Analysis (GNIA) was performed using ABAQUS, to compute the nonlinear equilibrium path for a given initial imperfection in the geometry. The numerical technique used for incremental analysis is that due to Riks (1972, 1979).

The shape of the imperfection was assumed to be the same as the eigenmode shown in Figure 2, and the maximum amplitude was scaled by means of a parameter ξ. The amplitude of the maximum deviations with respect to the cylindrical geometry were adopted as $\xi/t_1 = 1$, $\xi/t_1 = 2$, and $\xi/t_1 = 2.5$. The equilibrium path computed in each case is shown in Figure 3(a), and the maximum load λ^M reached along the path is recorded in each case. The equilibrium paths for $\xi/t_1 = 1$ and $\xi/t_1 = 2$ reach a maximum and then there is a small decrease in the path (equilibrium is only possible for values lower than λ^M). For $\xi/t_1 = 2.5$, on the other hand, the path exhibits an inflection point at λ^M. For this reason, imperfection sensitivity has only been investigated up to $\xi/t_1 = 2.5$ for this case.

The deflected shapes of the shell for $\xi/t_1 = 1$ and for $\xi/t_1 = 2.5$ are shown in Figure 4. Fourteen circumferential waves (i = 14) were obtained in both

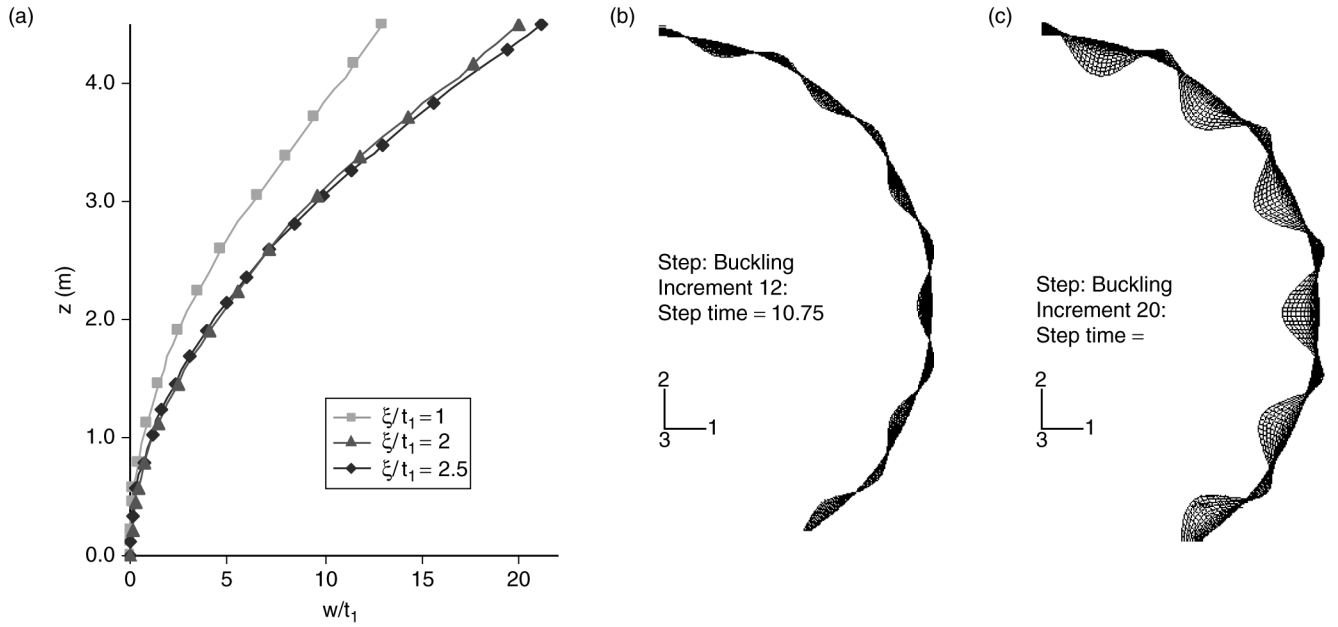

Figure 4. Deflected shape at the maximum load, for the shell of Figure 1, computed using nonlinear analysis: (a)in the longitudinal direction; (b) in the circumferential direction for $\xi/t_1 = 1$; (c) in the circumferential direction for $\xi/t_1 = 2.5$

Table 1. Summary of results from the geometrical nonlinear analysis

Imperfection amplitude	Maximum load λ^M [kN/m^2]	Knock-down factor η
$\xi/t_1 = 1$	1.437	0.78
$\xi/t_1 = 2$	1.257	0.68
$\xi/t_1 = 2.5$	1.228	0.66

eigenvalue and nonlinear analyses, with larger displacements towards the inside in the case of the shell with the largest imperfection.

It may be seen from Figure 3(a) that there is a significant drop in the maximum load that the shell can take from the classical value λ^C to the maximum value λ^M and this can be highlighted by defining a knock-down parameter $\eta = \lambda^M/\lambda^C$, which is listed in Table 1. The imperfection-sensitivity curve [Figure 3(b)] shows a drop in the maximum buckling capacity of the shell. A lower bound computed via nonlinear analysis can be estimated using $\xi/t_1 = 2.5$, in which case the knock-down factor becomes $\eta = 0.66$ for this particular shell.

2.2. Energy Contributions

In a RSA it is important to investigate the structure at the classical critical load level and compute the strain energy contributed by each shell component. In a classical bifurcation analysis, the modes are identified by the number of waves i in the circumferential direction, as shown in Figure 2. Separate energy contributions are here computed for each mode obtained, and the results are plotted in Figure 5. This type of plot has been employed in a number of works to illustrate the modal strain energy as a function of the circumferential wave number for a given meridional

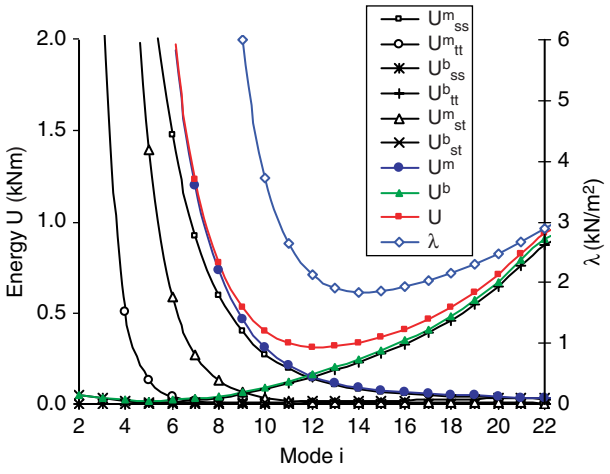

Figure 5. Modal energy components for different circumferential modes i for the structure of Figure 1

deflection. Since it represents the mode for the lowest critical buckling pressure a mode with one half wave in the meridional direction (j = 1) is usually represented in shells simply supported at both edges, whereas a cantilever-type deflection (as indicated in Figure 4) is used in this section for a clamped-free shell.

It may be seen that for modes with a small number of waves (i < 8), there are large contributions derived from membrane action, and they decrease with i, becoming negligible for i > 20. Bending contributions, on the other hand, are large for modes with a large number of waves in the circumferential direction. At the lowest total strain energy (i = 12), the membrane and bending contributions provide the same contributions.

The specific contributions of meridional, circumferential, and tangential components due to membrane and bending action are also plotted in Figure 5. At the critical state, the meridional membrane component (U^m_{ss}) accounts for 92% of the membrane energy of the shell; the second largest component is due to the membrane shear action, U^m_{st}, contributing 7%; whereas the circumferential membrane component U^m_{tt} is very small.

All membrane and bending components to the strain energy of the shell have positive values, i.e. they contribute to the stability of the shell. This trend is similar to what has been observed in pressurized cylinders with uniform thickness. Based on previous experience, it seem reasonable to use the same line of reasoning as in shells with uniform thickness and concentrate on the effect of eliminating part or all membrane energy contributions, based on the hypothesis that they will be eroded by the coupling between imperfections and modes (Croll 1995). However, there is some uncertainty in this case regarding what terms should be eliminated (some or all) in the membrane strain contribution to the eigenproblem of Eqn 3, and also about what region of the shell should be affected by such reduction.

2.3. Homogeneous Stiffness Reduction in the Bifurcation Analysis

The formulation of the RSA has already been discussed in other works (Batista and Croll 1979; Yamada and Croll 1993; and others), in which some of the stabilizing components to the stiffness of the shell are eliminated in the eigenvalue problem. The approach has been implemented in this investigation in two different ways: one through the elimination of components in the complete shell (called Homogeneous Stiffness Reduction), and another in which a reduction of membrane stiffness is limited to the thinnest part of the shell.

A direct application of the RSA in the present case is the elimination of the membrane components of the complete shell. To better understand the behavior of the shell with reductions in the thickness, first the meridional membrane component (U^m_{ss}) was eliminated; second, the membrane shear (U^m_{st}) components were eliminated; and finally, all the membrane contributions (U^m) were neglected. The reduced stiffness eigenvalues λ^* associated with mode i = 14 are shown in Table 2 together with the knock-down factor $\eta^* = \lambda^*/\lambda^C$.

The results do not show changes if either U^m_{ss} alone or U^m_{ss} and U^m_{st} are eliminated (both cases leading to $\eta^* = 0.64$), but some differences in eigenvalues are detected if the complete U^m is neglected ($\eta^* = 0.56$). However, the main differences are found in the eigenvectors, as shown in Figure 7(a). Elimination of just the meridional component (or the membrane shear components) lead to typical cantilever modes; however, an inadequate representation of the mode is obtained by complete elimination of the membrane strain energy in the reduced eigen-problem.

2.4. Selective Stiffness Reduction in the Bifurcation Analysis

An alternative analysis is to apply a selective stiffness reduction by eliminating only the membrane components associated with that region of the shell with small thickness t_1. For the case initially considered, the resulting eigenvalues are denoted by λ^{**} in Table 2, and the knock-down factors are $\eta^{**} = \lambda^{**}/\lambda^C$. It may be seen that the results of η^* and η^{**} are very similar, and the same values are also obtained if the spectra of critical loads for different modes are computed, as shown in Figure 6. Notice that these values ($\eta^* = \eta^{**} = 0.64$) are a lower bound to the load factor obtained using geometrically nonlinear analysis, $\eta = 0.66$.

Again, the solutions obtained using the complete elimination of Um do not provide a good estimate of the buckling modes. The shape of the deflected meridian is shown in Figure 7(a) for models in which the stiffness is reduced in the top-half of the shell, and it may be seen that the complete elimination of the membrane contribution leads to a deflected meridian with a shape

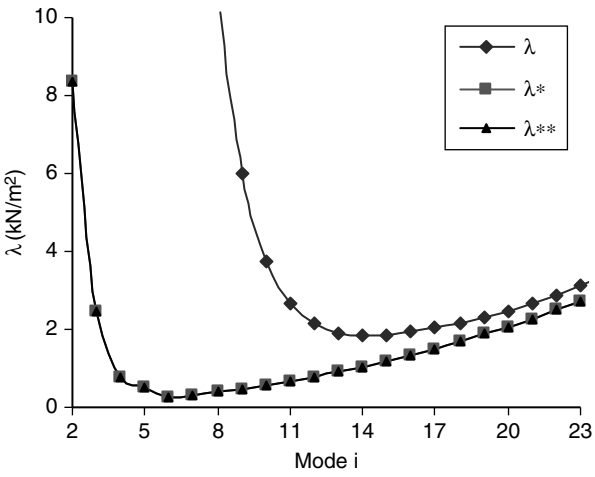

Figure 6. Classical critical loads for: (a) Full stiffness (λ); (b) Homogeneous RSA (λ^*), (c) Selective RSA (λ^{**})

very different from that computed via nonlinear analysis, Figure 5(a). A better approximation is obtained through the use of a model in which only the meridional (or membrane shear) components are eliminated. Although the numerical contribution of the circumferential stiffness is very small, its complete elimination yields a distorted shape that does not correctly represent the buckling mode.

In order to illustrate the type of lower bound computed using the present methodology, the results for the tank of Figure 1 have been compared with those of GNIA nonlinear analysis for different forms of imperfections and are plotted in Figure 8. Using an asymptotic analysis (in the vicinity of a critical state) Koiter considered an eigenmode affine imperfection shape, and this is closely correlated with the imperfections sensitivity of the shell at the initial postcritical path using small imperfections. However, there is no warranty that this would be the worst imperfection profile, especially when large amplitude imperfections are considered.

The forms of imperfections included in the present analysis are the shape of the lowest eigenvector in the classical analysis, the shape modes associated with the second and third eigenvalues, and a localized mode (as described in Holst *et al*. 2000) acting at the junction

Table 2. Reduced stiffness analysis using complete elimination of components in the complete shell or just in the zone with the smallest thickness

Energy terms eliminated	Homogeneous reduction		Selective reduction	
	λ^* [kN/m²]	η^*	λ^{**} [kN/m²]	η^{**}
U^m_{ss}	1.177	0.64	1.186	0.64
U^m_{ss}, U^m_{st}	1.177	0.64	1.177	0.64
U^m	1.038	0.56	1.023	0.55

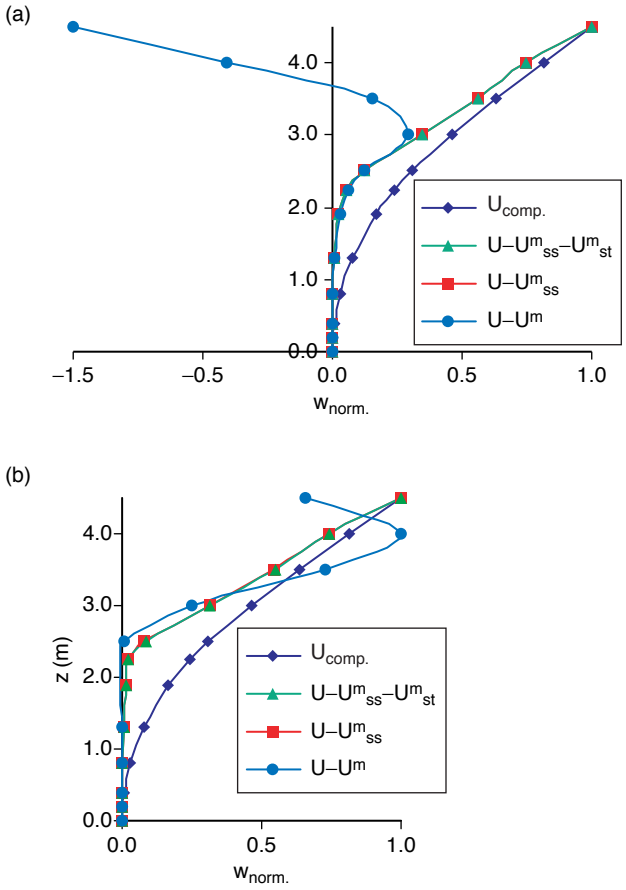

Figure 7. Buckling modes computed with reduced membrane contribution: (a) homogeneous in the complete shell; (b) selective in the zone of smaller thickness

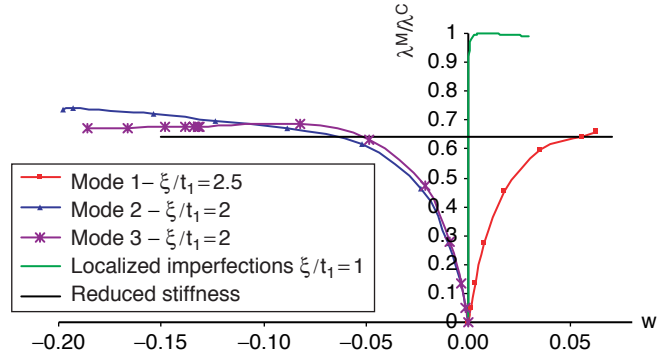

Figure 8. Non-Linear equilibrium paths with different imperfection shapes for the structure of Figure 1

between the parts of the shell with different thicknesses. The plots show the largest imperfection amplitude for which a maximum is reached in the equilibrium path. The results show that the present RSA is a lower bound to the nonlinear equilibrium paths including imperfections. Of course this group of imperfections employed in the analysis does not cover all possible imperfection shapes, but is indicative of the type of expected response for this class of shells.

2.5. Analysis of a Real Tank

A second tank with three different thicknesses designed using API 650 (1988), shown in Figure 9, was investigated. This tank has been previously studied by Sosa *et al.* (2006), leading to a classical critical load $\lambda^c = 884$ Pa and i = 16 circumferential waves.

A homogeneous RSA was first used by affecting the complete structure. With elimination of just the meridional membrane energy component, the reduced eigenvalue is $\lambda^* = 692$ Pa, with i = 16, so that the knock-down factor is $\eta = 0.78$. This is almost the same eigenvalue obtained if the tangential membrane energy is also neglected. A complete elimination of the membrane energy, on the other hand, yields the lower value of $\lambda^* = 621$ Pa ($\eta = 0.70$), and again the mode shape differs significantly from the classical eigenmode. The results from GNIA model produced a knock-down factor $\eta = 0.78$, which is almost coincident with our reduced stiffness value.

The same tank was analyzed using selective RSA, leading to $\lambda^{**} = 704$ Pa ($\eta^{**} = 0.79$) when U^m_{ss} or $U^m_{ss} + U^m_{st}$ were eliminated. The elimination of all U^m leads to $\lambda^{**} = 621$ Pa, Thus, homogeneous and selective approaches to reduce the stiffness produce virtually the same lower bounds for this problem.

Figure 10 shows equilibrium paths obtained using GNIA implemented in ABAQUS. Four different imperfections were considered in this case, namely the

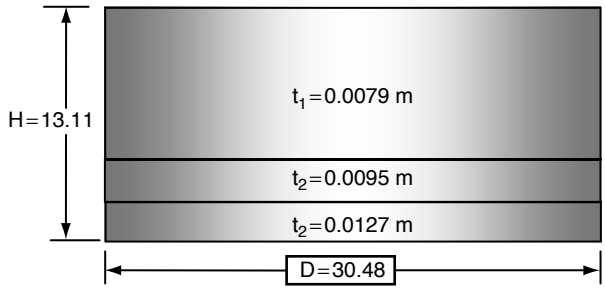

Figure 9. Metal tank open at the top ($D/t_1 = 3828$, $H/D = 0.43$)

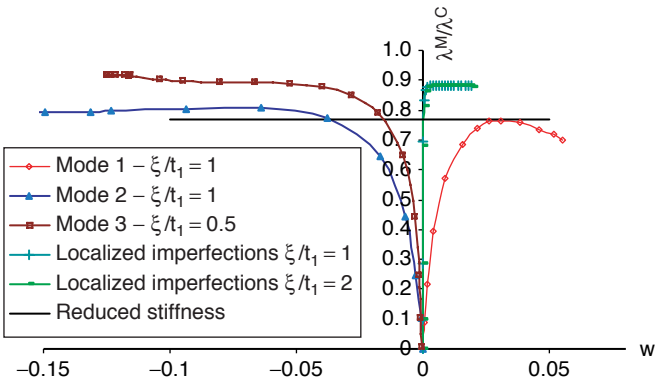

Figure 10. Non-Linear equilibrium paths with different imperfection shapes for the structure of Figure 8

shape associated to the lowest eigenvalue, and to the two following eigenvalues, and a localized mode. From the present results, the knock-down factor ($\eta^{**} = 0.79$) from selective RSA can be considered as a lower bound for different imperfection shapes.

3. TANKS WITH STEPWISE THICKNESS CHANGES AND CONICAL ROOF

The presence of a roof introduces important differences in the value of modal energy components in the structures of storage tanks, because there may be modes affecting just the cylindrical part or the roof of the tank. To illustrate the RSA, tanks with conical roof have been investigated following Sosa *et al.* (2006), who considered six configurations with stepwise variable thicknesses, assuming the same diameter and conical roof but with different heights (Figure 11). The designs were made using API 650 (1988). The conical roof had 3/16 slope, thickness 7mm and was reinforced with a frame of 32 beams.

Under uniform external pressure, buckling modes involve deflections mainly in the cylindrical part of the tank. Analyses of the classical critical pressures and associated modes are shown in Figure 12 for tanks with

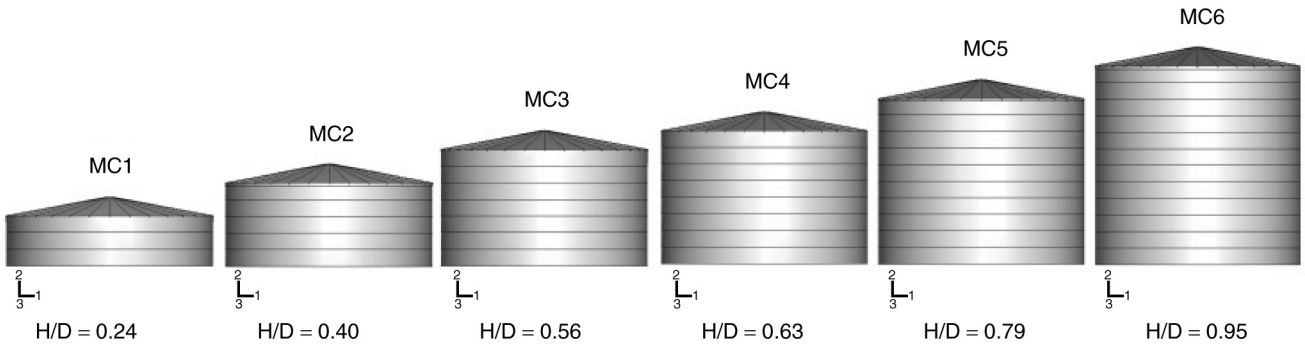

Figure 11. Geometry of investigated shells with conical roofs

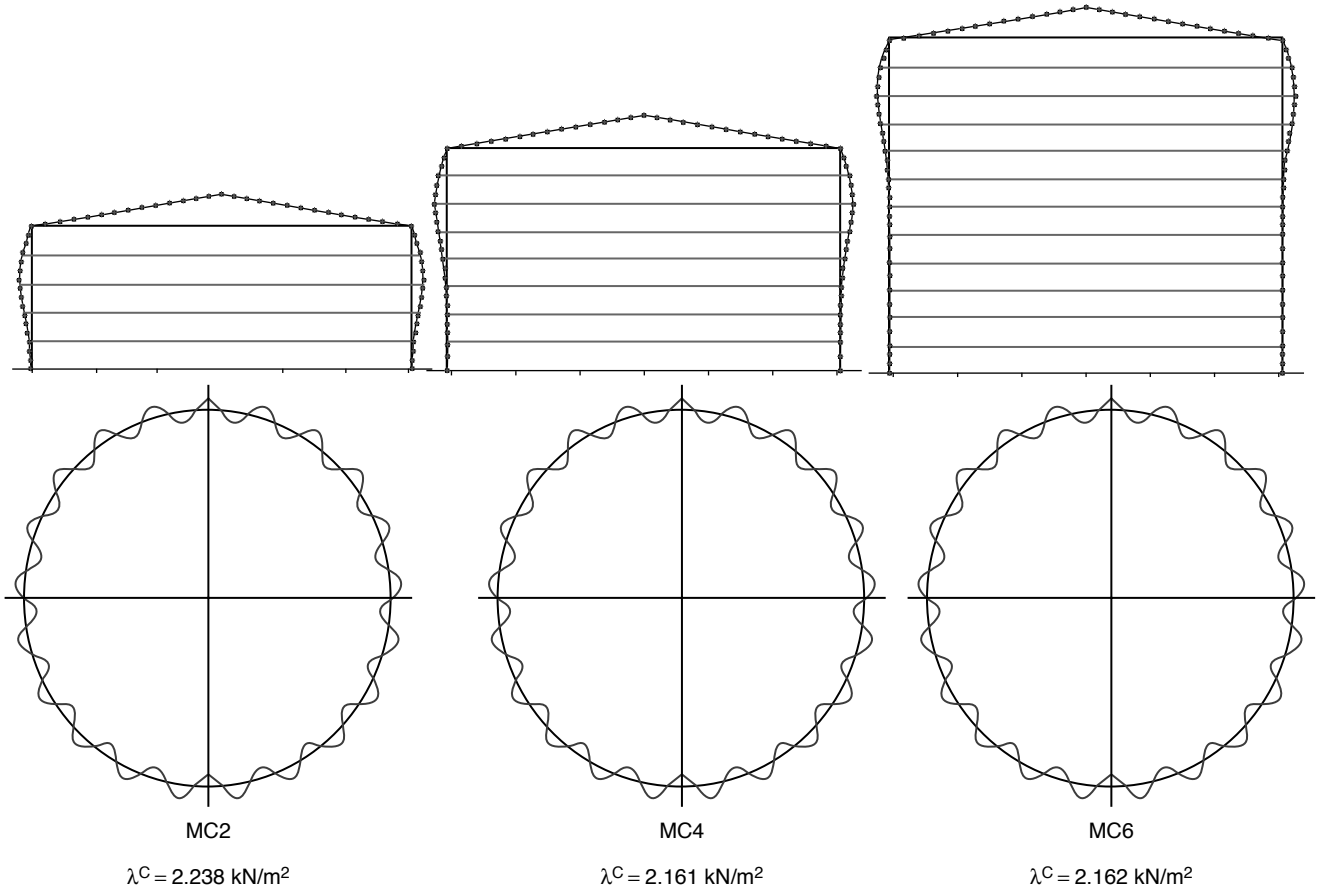

Figure 12. Buckling modes under internal vacuum for the tanks shown in Figure 11

Table 3. Thickness of tanks shown in Figure 9

Shell course	MC1 t [m]	MC2 t [m]	MC3 t [m]	MC4 t [m]	MC5 t [m]	MC6 t [m]
1	0.0095	0.0127	0.0175	0.0206	0.0254	0.0286
2	0.0079	0.0111	0.0159	0.0175	0.0222	0.0254
3	0.0079	0.0079	0.0127	0.0159	0.0206	0.0254
4		0.0079	0.0111	0.0127	0.0175	0.0222
5		0.0079	0.0095	0.0111	0.0159	0.0206
6			0.0079	0.0079	0.0127	0.0191
7			0.0079	0.0079	0.0111	0.0159
8				0.0079	0.0079	0.0127
9					0.0079	0.0111
10					0.0079	0.0079
11						0.0079
12						0.0079

H/D = 0.40, 0.63, and 0.95, for which the thicknesses are listed in Table 3. The modes are similar in each case shown in Figure 12, in the sense that they develop out-of-plane deflections in the top part of the shell and do not have displacements at the bottom half in the taller tank (H/D = 0.95). Unlike the open tanks of the previous section the out-of-plane deflections within the cylindrical wall are restrained at the top by the conical roof. Further, they all have i = 21 circumferential waves. Notice that the classical pressure is the same for the tanks with H/D = 0.63 and 0.95 (because buckling is here controlled by the thinner upper courses), and it is higher for the shorter tank with H/D = 0.40 (because the shell length is of the same order as the buckling mode in taller tanks). Several authors have considered the influence of changing the height of a cylindrical shell under external pressure, notably Greiner (2004), who considered a clamped-simply supported cylinder and found that the same mode was present in all cases, since the buckling problem is dominated by the thinner part of the shell in that case.

Using a geometrically nonlinear analysis, the results of Sosa *et al*. (2006) showed that they all have the same imperfection sensitivity. The knock-down factor computed via GNIA using the first eigenmode is $\eta = 0.73$ in all six cases.

An investigation of the modal strain energy contributions is shown in Figure 13 for three tanks. It is clear that the complete strain energy does not show a unique minimum as in the case of the cantilever shell, but it has two local minimum values due to the interaction between the two shell components (cylinder and cone). With increasing values of H/D, the energy tends to approach the distributions associated with the individual shell components. For modes with a low number of circumferential waves, membrane action of the cylinder dominates, but it decays with the increasing number of waves, until a first minimum is reached in the strain energy.

A new increase in membrane components of the strain energy occurs for mode 15, which is accompanied by decay in the bending action. A second minimum in the strain energy is exhibited at higher wave number modes.

A comparison of results computed with the reduced stiffness approach is shown in Table 4 for three tank configurations, with H/D = 0.40, 0.63, and 0.95. The reduction has been limited to the zone of smaller shell

Table 4. Results of RSA for the tanks shown in Figure 9

Tank		$U-U^m_{ss}$ selective		$U-U^m_{ss}-U^m_{st}$ selective		$U-U^m_{ss}$ homogeneous		$U-U^m_{ss}-U^m_{st}$ homogeneous
MC2	λ^{**}	1586		1583	λ^{*}	1567		1566
	η^{**}		0.71		η^{*}		0.70	
MC4	λ^{**}	1365		1361	λ^{*}	1340		1340
	η^{**}		0.63		η^{*}		0.62	
MC6	λ^{**}	1365		1361	λ^{*}	1340		1340
	η^{**}		0.63		η^{*}		0.62	

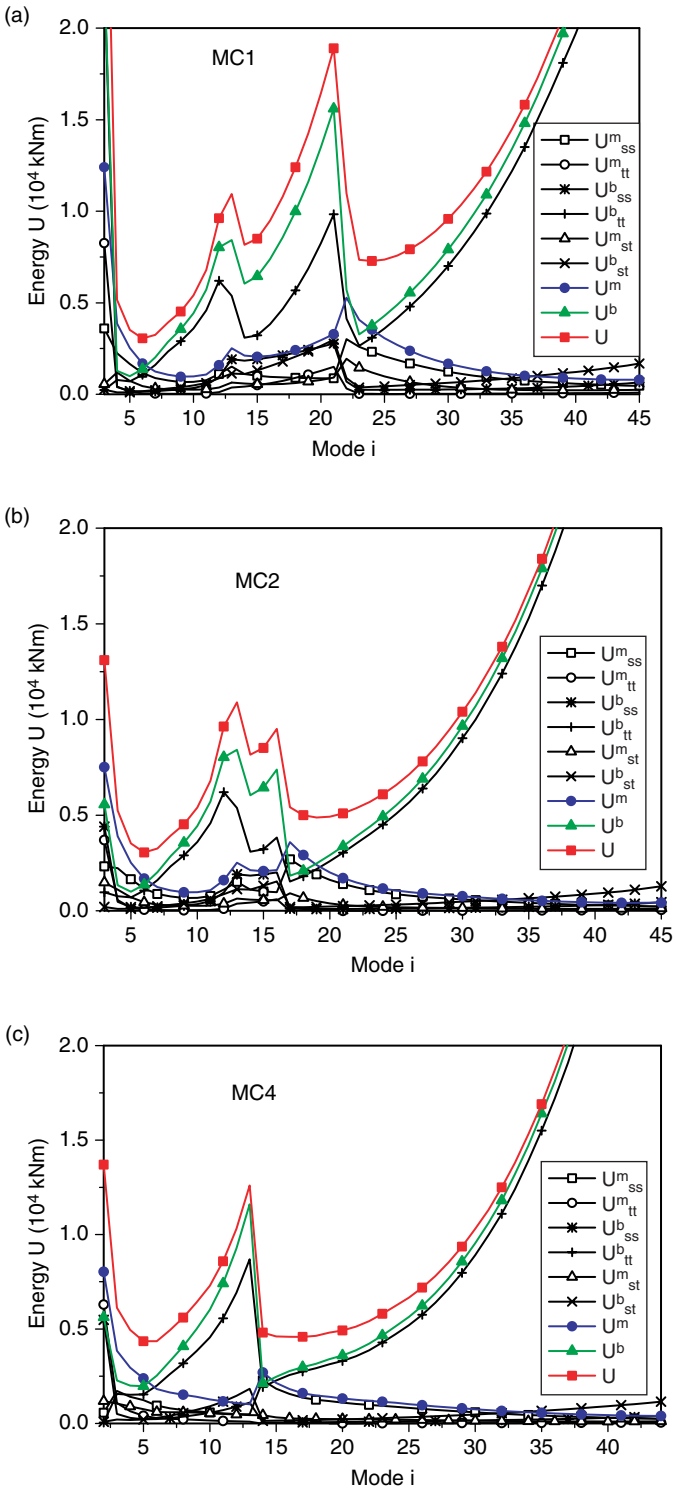

Figure 13. Modal strain energy for tanks shown in Figure 11: (a) H/D = 0.24; (b) H/D = 0.4; (c) H/D = 0.63

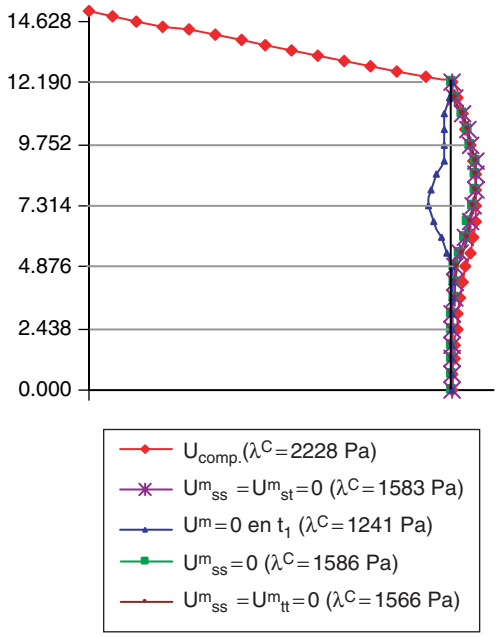

Figure 14. Results from selective RSA: showing eigenmodes for model MC2

thickness (selective RSA), which includes the top three courses in all cases. The approach followed was to apply the stiffness reduction in the zone for which there are significant displacements in the shape of the eigenvector associated to the lowest eigenvalue. In this case, this corresponds to the top three courses of the shell. An elimination of the meridional membrane energy component results in a know-down factor $\eta^{**} = 0.71$ for the shortest tank and $\eta^{**} = 0.63$ for the other two. This last value is lower than the values computed using GNIA, for which $\eta = 0.73$ was obtained. A reduction in the complete height of the shell (homogeneous RSA) leads to similar results for knock-down factor (η^*), as shown in Table 4.

The buckling modes identified with this technique are shown in Figure 14 for the short tank with H/D = 0.40. The mode is coincident with what is expected from an analysis without reduction. However, it may be seen that if the complete membrane energy is eliminated, then the associated mode computed is incorrect.

The results computed using the present RSA approach have been compared with those from a GNIA model using different imperfection shapes. The results for imperfections with the shape of the eigenmodes associated to the lowest three eigenvalues in the classical analysis have been considered, together with localized imperfections introduced in two ways: at the thickness changes and at the course changes. The most critical imperfection shape in this case is the shape associated to the lowest eigenvalue.

4. COMPARISON WITH FULL SCALE TESTING

An unusual situation in this engineering problem is that full-scale experiments of various tanks (some of them with stepwise variable thickness) have been reported in the literature (Hornung and Saal 2002). The tests were

performed by producing internal vacuum in cylindrical tanks with shallow spherical dome roofs. The tests were continued until collapse occurred; however, the authors also identified when the first signs of buckling were observed and the number of circumferential waves in the deflected mode at failure. Information of the imperfections is also available for some of the tested tanks.

4.1. Results for Tank ME1

One of the small tanks (for which data was reported) had D = 10 m, H = 13.29 m and a constant thickness t = 0.01 m (H/D = 1.33, D/t = 1000). Values of E = 206 GPa and Poisson's ratio 0.3 were employed in the computations.

According to the authors, buckling was first recorded at 11.6 kPa with a mode approximating i = 6; whereas collapse occurred at 11.8 kPa with i = 5.

For such data, our computations of a classical LBA analysis using ALREF produced a λ^c = 16.1 kPa with i = 9, which is much higher than the load attained in the experiments. At the critical state the meridional membrane component contributed 88% of the membrane strain energy, with a contribution of the tangential component of 11.3% and of the circumferential component of 0.6%.

A homogeneous reduction in the meridional membrane stiffness leads to 12.66 kPa or η^* = 0.78, which is consistent with a GNIA of the same shell. This value is close but higher than the pressure 11.6 kPa reported from the experiments.

No indication is given about the imperfections in the tank tested. The boundary conditions and elastic modulus that would best reflect those in the experiments are again unknown to the present authors. Other effects could be present in the real tank, such as corrosion of the material or material aging, which could perhaps be responsible for the 8% difference between experiments and reduced stiffness computations.

4.2. Results for Tank ME4

A second tank was investigated with D = 11.5 m, H = 10 m, in which the top four courses had t_1 = 5 mm and it was increased to 6 mm and 7 mm in the two lower courses (H/D = 0.87, D/t_1 = 2300). Very large imperfections were measured in this tank, of the order of ξ/t_1 = 6.6. The first signs of buckling were recorded at λ = 1.36 kPa with i = 7, and the deflections increased forming column-like segments that collapsed at λ = 2.78 kPa.

Our computations showed a classical LBA leading to λ^c = 3.04 kPa with i = 13. A nonlinear analysis (GNIA) using ABAQUS is shown in Figure 16. For large imperfections this is a case in which deflections did not reach an inflection point and it is not possible to identify a maximum load. The selective RSA with elimination of the meridional membrane component in the strain energy affecting just t_1 predicted a value λ^{**} = 2.1 kPa, with η^{**} = 0.69. As shown in Figure 16 this value is a lower bound with respect to a nonlinear analysis with imperfections of the order of the thickness, even considering different imperfection shapes, as indicated in Figure 17.

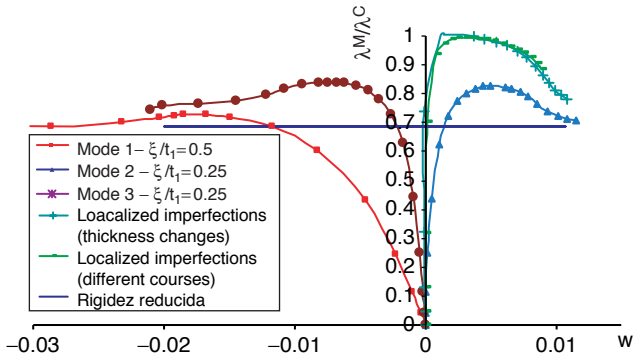

Figure 15. Non-Linear equilibrium paths with different imperfection shapes for the structure identified as MC2

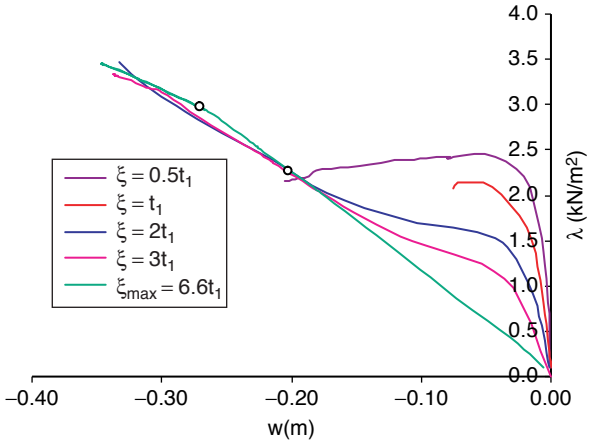

Figure 16. GNIA for tank with H/D = 0.87 and D/t_1 = 2300 reported by Hornung and Saal (2002)

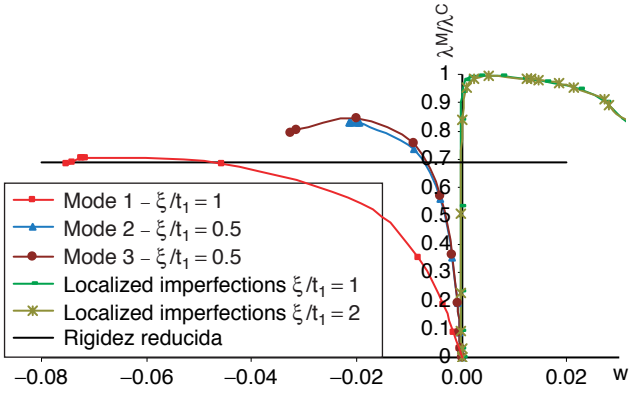

Figure 17. Non-Linear equilibrium paths with different imperfection shapes for the structure identified as ME4

5. CONCLUSIONS

The developments and implementations reported in this paper show that it is possible to extend the reduced stiffness approach to shell buckling problems with stepwise changes in the thickness. The importance of this topic is associated with the generalized construction of oil storage tanks with variable thickness, which should be designed to resist external pressures. The paper attempts to illustrate that there are several ways in which the implementation may be conceived, depending on the area in which the reduction takes place and on the specific form in which the stiffness is reduced. The results were limited to uniform external pressure, and were validated by comparisons with imperfection-sensitivity studies performed using geometrically nonlinear analysis.

In the homogeneous reduction, the stiffness reduction is applied on the complete domain of the shell, thus equally affecting shell segments with different thicknesses. In the selective reduction, only the top thinner segments are affected by the proposed methodology. The two methodologies produced similar results with minor differences and the conclusion is that both could be used in a practical analysis.

The answer to the question of what membrane terms should be neglected in order to have an adequate RSA is not dominated by the reduced eigenvalues but by their associated eigenvectors. All techniques provide acceptable lower bounds in terms of reduced critical loads, but the associated modes are not always a good representation of the modes captured by the nonlinear computations. In the complete elimination of membrane energy, the modes become distorted, showing spurious curvatures near to the top of the shell. Thus, elimination of just the meridional membrane component seems to be a good way to implement lower bounds using a RSA.

Comparisons with some tanks tested up to failure in Germany under the action of internal vacuum have also been modeled using RSA. Limited information was reported in the literature concerning imperfections and material properties, but large amplitude imperfections were reported in some cases and corrosion could have been present in such old tanks, thus reducing the effective shell thickness. This may be a factor in attempting to understand differences between collapse loads measured in the field and the present computational model.

Finally, it should be noted that the specific terms that are eliminated from the reduced stiffness analysis depend on the geometric configuration of the shell (either cylindrical, spherical, etc.) and on the loading considered (uniform external pressure, wind pressure, axial load). The scope of this paper was limited to configurations of storage tanks under external pressure.

ACKNOWLEDGMENTS

The authors thank the contribution of Fernando Flores who developed the original version of the software ALREF. This work was supported by grants from the National University of Comahue, from FONCYT, and from the National University of Cordoba, in Argentina. LAG was supported by the Science Research Council of Argentina (CONICET) during this research.

REFERENCES

Abaqus (2002). *User's Manuals,* Version 6.3, Hibbitt, Karlsson and Sorensen Inc., Rhode Island.

API Standard 650 (1988). *Welded Steel Tanks for Oil Storage*, American Petroleum Institute, Washington, D.C.

Batista, R.C. and Croll, J.G.A. (1979). "A design approach for unstiffened cylindrical shells under external pressure", *Proceedings of International Conference on Thin-Walled Structures*, University of Stratchclyde, Crosby Lockwood, Glasgow.

Croll, J.G.A. (1975). "Towards simple estimates of shell buckling loads", *Der Stahlbau*, Vol. 8, pp. 243.

Croll, J.G.A. (1995). "Towards a rationally based elastic-plastic shell buckling design methodology", *Thin Walled Structures*, Vol. 23, No. 1–4, pp. 67–84.

Donnell, L.H. (1934). "A new methodology for the buckling of thin cylinders under axial compression and bending", *ASME Journal of Applied Mechanics*, Vol. 56, pp. 795–806.

Flores, F.G. and Godoy, L.A. (1991). "Instability of shells of revolution using ALREF: Studies for wind loaded shells", In *Buckling of Shells in Land, in the Sea and in the Air*, Elsevier Applied Science, Oxford, pp. 213–222.

Greiner, R. (2004). "Cylindrical shells under uniform external pressure", Chapter 5 in *Buckling of Thin Metal Shells*, J.G. Teng and J.M. Rotter, eds., Spon Press, London.

Greiner, R. and Yang, Y. (1996). "Effect of imperfections on the buckling strength of cylinders with stepped wall thickness under axial loads", *Proceedings of the International Workshop on Imperfections in Metal Silos*, Lyon, France, pp. 77–86.

Federal Emergency Management Agency (FEMA). (2003). *HAZUS-MH, Multihazard Loss Estimation Methodology*, FEMA, Department of Homeland Security, Washington, DC.

Holst, J.M.F.G., Rotter, J.M. and Calladine, C.R. (2000), "Imperfections and buckling in cylindrical shells with consistent residual stresses", *Journal of Constructional Steel Research*, Vol. 54, No. 2, pp. 265–282.

Hornung, U. and Saal, H. (2002). "Buckling loads of tank shells with imperfections", *International Journal of Non-Linear Mechanics*, Vol. 37, No. 4–5, pp. 605–621.

Jaca, R.C., Godoy, L.A., Flores, F.G. and Croll, J.G.A. (2007). "A reduced stiffness approach for the buckling of open cylindrical

tanks under wind loads", *Thin Walled Structures*, Vol. 45, No. 9, pp. 727–736.

Khanduri, A.C. and Morrow, G.C. (2003). "Vulnerability of buildings to windstorms and insurance loss estimation", *Journal of Wind Engineering and Industrial Aerodynamics*, Vol. 91, No. 4, pp. 455–467.

Resinger, F. and Greiner, R. (1982). *Buckling of Wind Loaded Cylindrical Shells-Application to Unstiffened and Ring-Stiffened Tanks*, Institut für Sthalbau, Holzbau und Flächentragwerke Technische Universität Graz, Austria, pp. 305–331.

Riks, E. (1979). "An incremental approach to the solution of snapping and buckling problems", *International Journal of Solids and Structures,* Vol. 15, No. 7, pp. 529–551.

Riks, E. (1972). "The application of Newton's method to the problem of elastic stability", *Journal of Applied Mechanics,* Vol. 39, No. 4, pp. 1060–1065.

Rotter, J.M. and Schmidt, H. (2008). *Buckling of Steel Shells: European Design Recommendations*, 5th Edition, European Convention for Constructional Steelwork, Mem Martins, Portugal.

Rotter, J.M. and Teng, J.G. (1989). "Elastic stability of lap-jointed cylinders", *Journal of Structural Engineering*, ASCE, Vol. 115, No. 3, pp. 683–697.

Sosa, E.M. and Godoy, L.A. (2007). "Análisis computacional del pandeo de paneles cilíndricos bajo presión uniforme", *Revista Int. Métodos Numéricos para Cálculo y Diseño en Ingeniería*, Vol. 23, No. 2, pp. 319–334.

Sosa, E.M., Godoy, L.A. and Croll, J.G.A. (2006). "Computation of lower-bound buckling loads using general-purpose finite element codes", *Computers and Structures*, Vol. 84, No. 29–30, pp. 1934–1945.

Trahair, N.S., Abel A., Ansourian, P., Irvine H.M. and Rotter, J.M. (1983). *Structural Design of Steel Beams for Bulk Solids*, Australian Institute of Steel Construction, Sydney.

Yamada, S. and Croll, J.G.A. (1993). "Buckling and postbuckling characteristics of pressure-loaded cylinders", *Journal of Applied Mechanics*, Vol. 60, No. 2, pp. 290–299.

Zienkiewicz, O.C. and Taylor, R. (2005). *The Finite Element Method for Solid and Structural Mechanics*, Elsevier, Oxford, UK.